GAS-COOLED REACTOR
ADVANCED REACTOR TECHNOLOGIES PROGRAM

July 16, 2024

Statistical modeling of the effect of microstructural heterogeneity on the irradiation behavior of TRISO fuel buffer layer

Yongfeng Zhang

Assistant Professor

University of Wisconsin Madison

DOE ART GCR Review Meeting

Hybrid Meeting at INL

July 16–18, 2024

Project information

- Title: Statistical modeling of the effect of microstructural heterogeneity on the irradiation behavior of TRISO fuel buffer layer
- ID: 20-19556
- PI: Yongfeng Zhang, University of Wisconsin Madison (UW)
- Co-Pis: Ramathasan Thevamaran (UW), Karim Ahmed (TAMU), Tyler Gerczak (ORNL), Wen Jiang (INL)
- Funding: $800,000
- Period: 10/1/2020 - 9/30/2023 (with NCE to 6/30/2024)

Outline

- **Background & objective**
- **Hypothesis**
- **Research design**
- **Accomplishments**
  - ▶ How do we describe buffer? matrix microstructure + porosity
  - ▶ How does buffer porosity affect its fracture behavior?
  - ▶ Irradiation induced changes in porosity and matrix microstructure
  - ▶ Unique mechanical properties of unirradiated buffer pyrocarbon
- **Outlook**
- **Summary**

Background & objective

- Buffer fracture is stochastic showing three different modes: Debonding (**A**), radial fracture (**B**), and partial debonding (**AB**), while mode **AB** leads to higher probability of failure.

- **Our objective is to answer:**
  - Why fracture is stochastic?
  - What governs the selection of fracture mode?
  - Can we control the fracture mode?

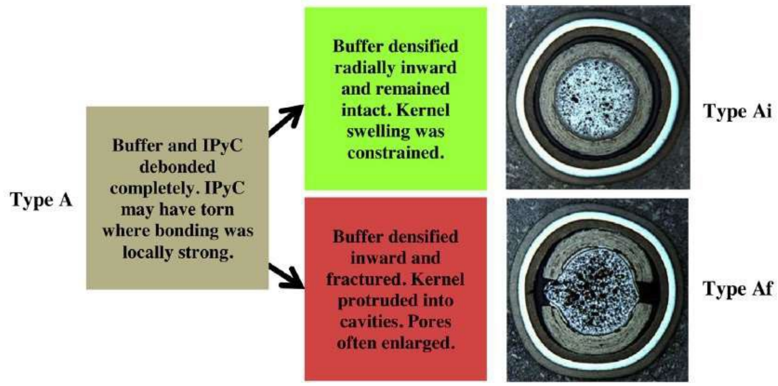

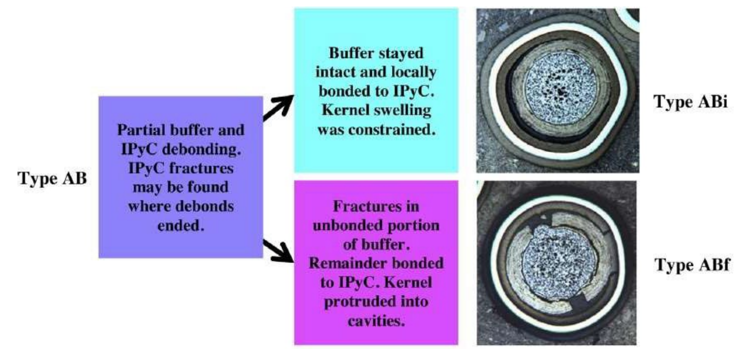

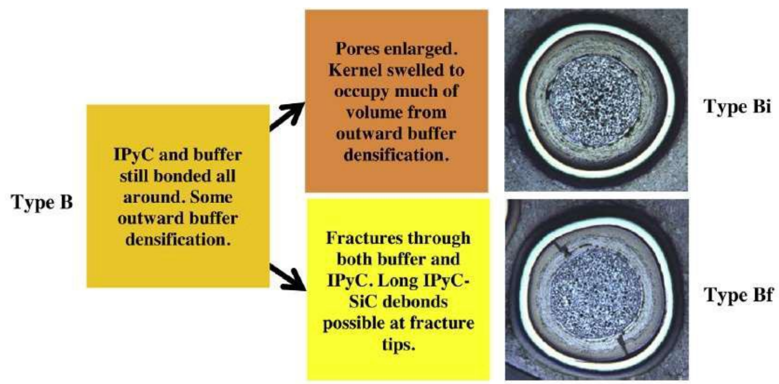

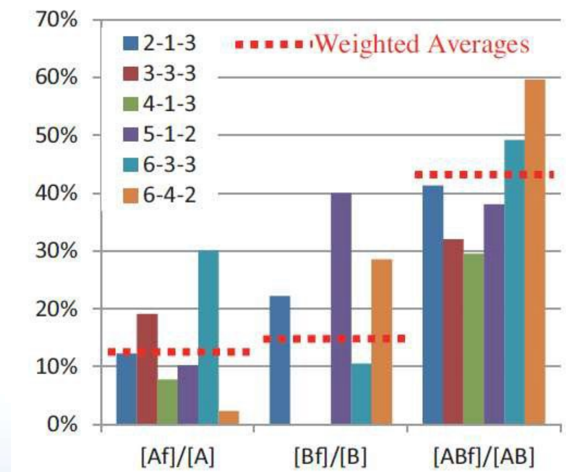

Ploger, S. A., Demkowicz, P. A., Hunn, J. D., & Kehn, J. S. (2014). Nuclear Engineering and Design, 271, 221-230

Hypothesis: The heterogeneous distribution of buffer porosity determines the initiation and propagation of buffer fracture.

Buffer porosity:

- Random distribution
- Local fluctuation
- Radially increasing
- Connectivity along tangential direction

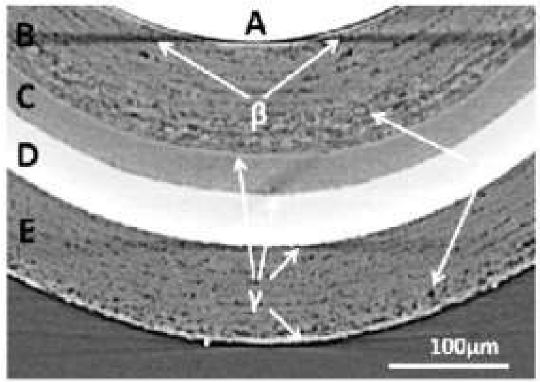

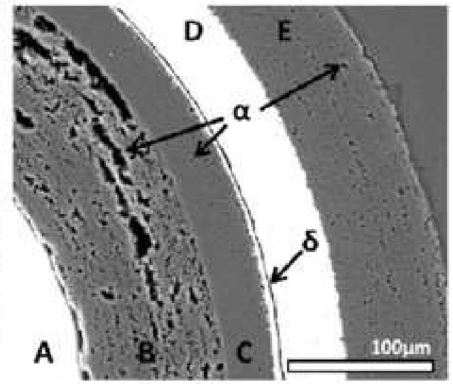

T. Lowe et al. JNM 461, 29-352015

J. D. Hales et al., J. Nucl. Mater. 443, 531–543, 2013.

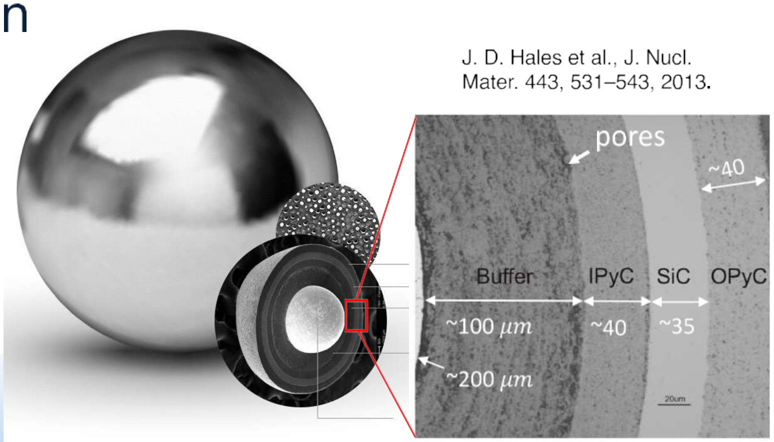

S. Liu et al. Front. Mater., 04 January 2023

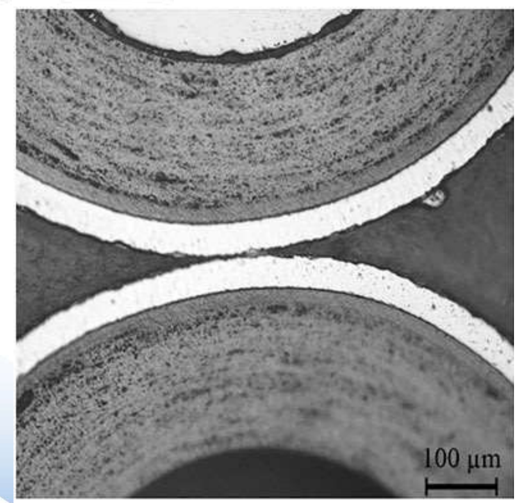

Research design

- What are the actual porosity in buffer and its spatial distribution?
- What's the atomic structure of buffer, which is a low density, non-textured pyrocarbon?
- How does porosity correlate with mechanical properties: moduli, toughness, etc.?
- How does porosity distribution affect the buffer fracture (tearing)?

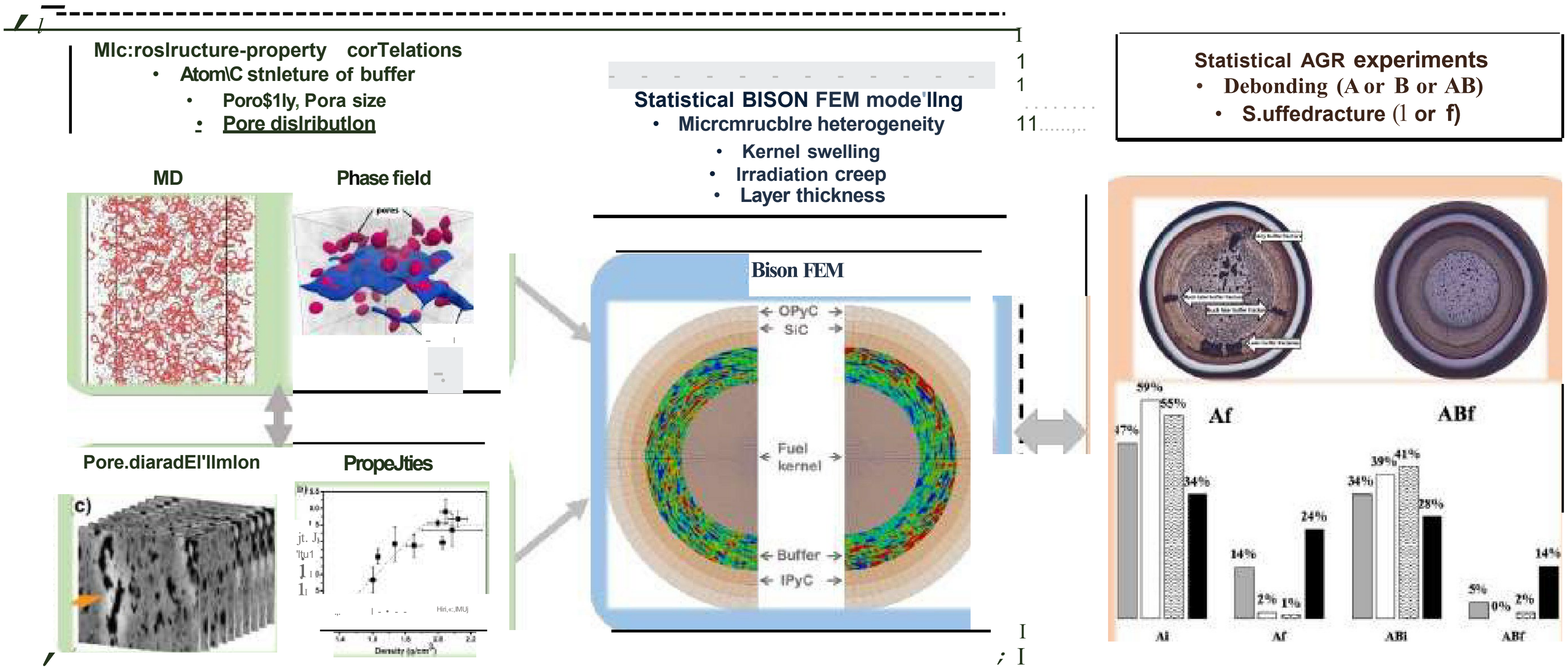

How do we describe buffer?

- **FIB-SEM characterization of buffer porosity**
  - *Griesbach et al. Microstructural heterogeneity of the buffer layer of TRISO nuclear fuel particles, JNM 574 (2022)*

1st place Winner of FY 2023 Innovations in Nuclear R&D Student Competition: Fuel Cycle Technologies

- **Atomistic simulations of pyrocarbon matrix**
  - *R. David et al. Correlations between atomic structure and elastic properties in low-density non-textured pyrocarbon (in preparation)*

Buffer porosity morphology in unirradiated TRISO buffer {surrogate particles)

A robust data analysis workflow is established incorporating artificial intelligence assisted pore identification and segmentation for porosity characterization of FIB-SEM image.

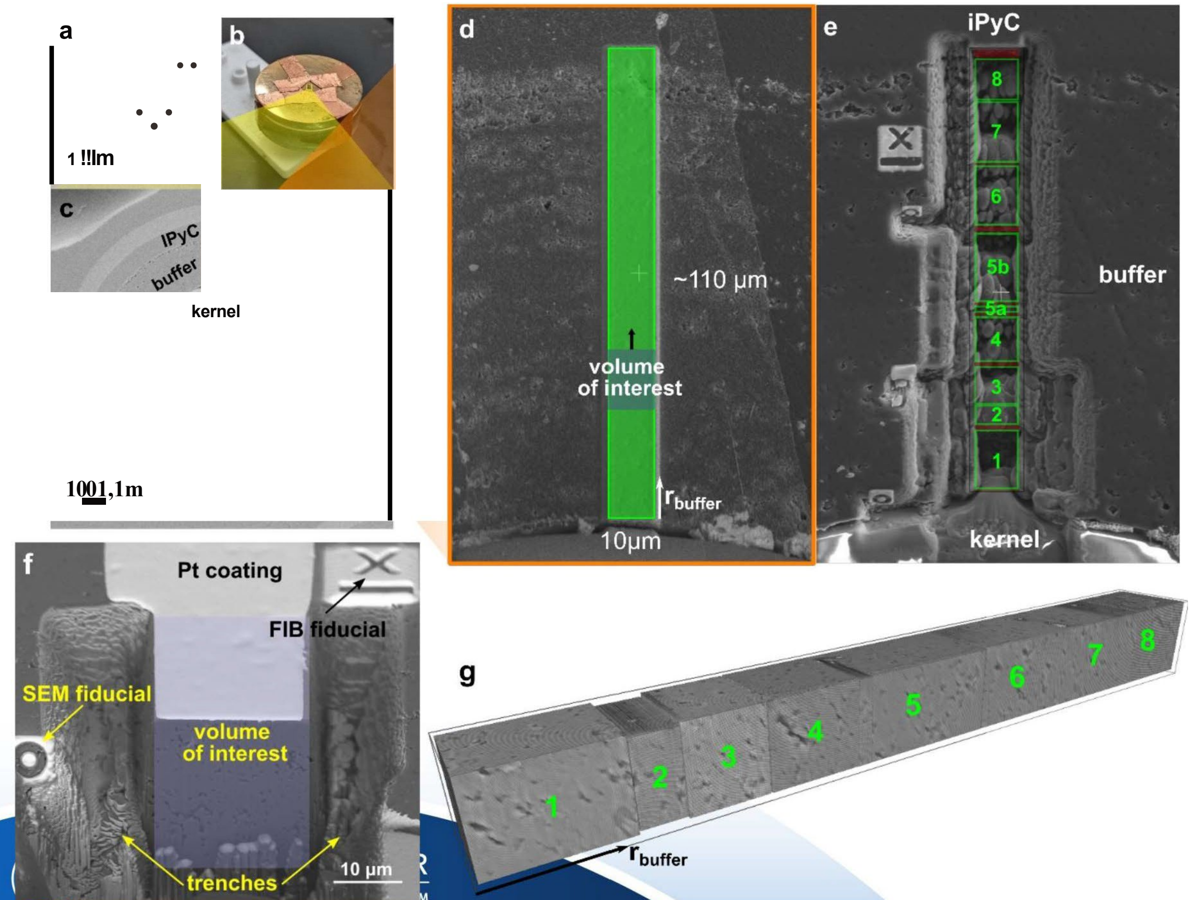

FIB-SEM tomography

- FEI Helios PFIB with 30 kV Xe plasma
- Scan volume: 1Ox1Ox10 μm^3
- Slice thickness: 50 nm
- Voxel size: 38x49x5Qnm^3

- Image processing and data analyses:
  - Avizo 9.5 and Dragonfly 2021.1
  - Deep learning segmentation

- 3D reconstruction

Buffer: low density pyrocarbon + randomly distributed pores

- **The Average buffer porosity is about 14% in reference to the 50% smeared theoretical density.**
- **Pores distribute randomly.**
- **Porosity increases radially.**
- **Porosity fluctuates locally.**
- Large pores ($>1 \mu m^3$) dominates the porosity albeit fewer of them.

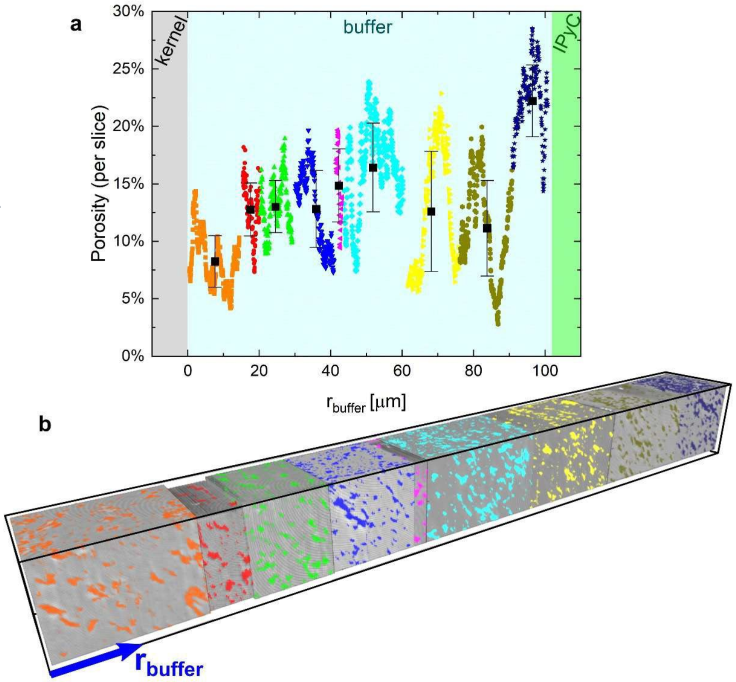

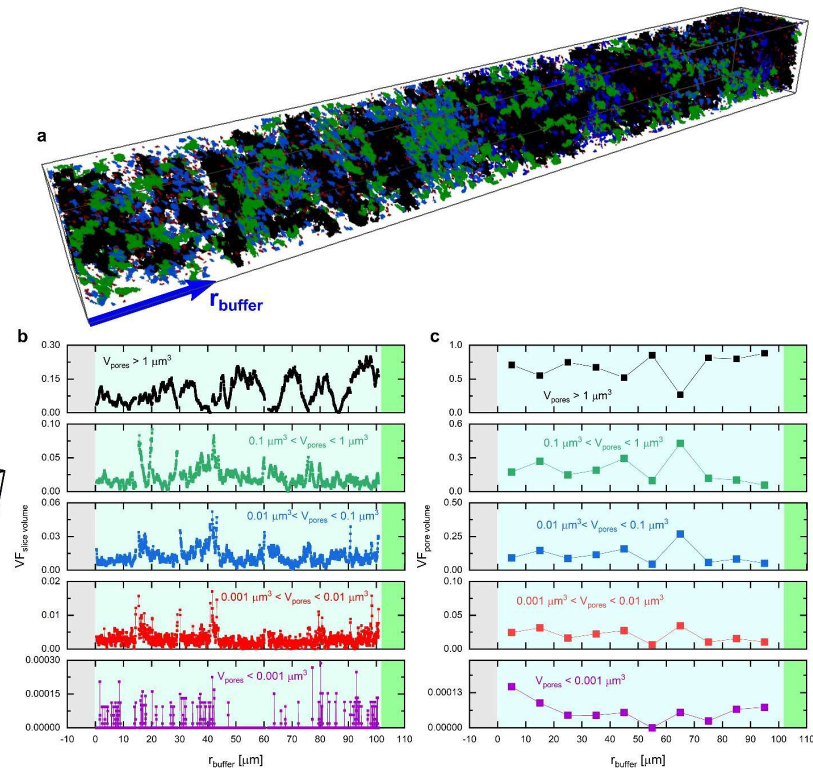

Buffer consists of low density pyrocarbon with 58% theoretical density and randomly distributed pores that give a total porosity of 14%.

Inter-particle (and radial direction) differences

- The radial porosity distribution varies upon the radial direction and from particle to particle
- However, the average porosity, magnitude of local fluctuation and radial gradient are similar.
- The radial increase of porosity is consistent with the fabrication procedure.
- The AGR-2 buffer displays a similar porosity distribution to that in surrogate particles.
- More characterizations (which are exoensive) are desired.

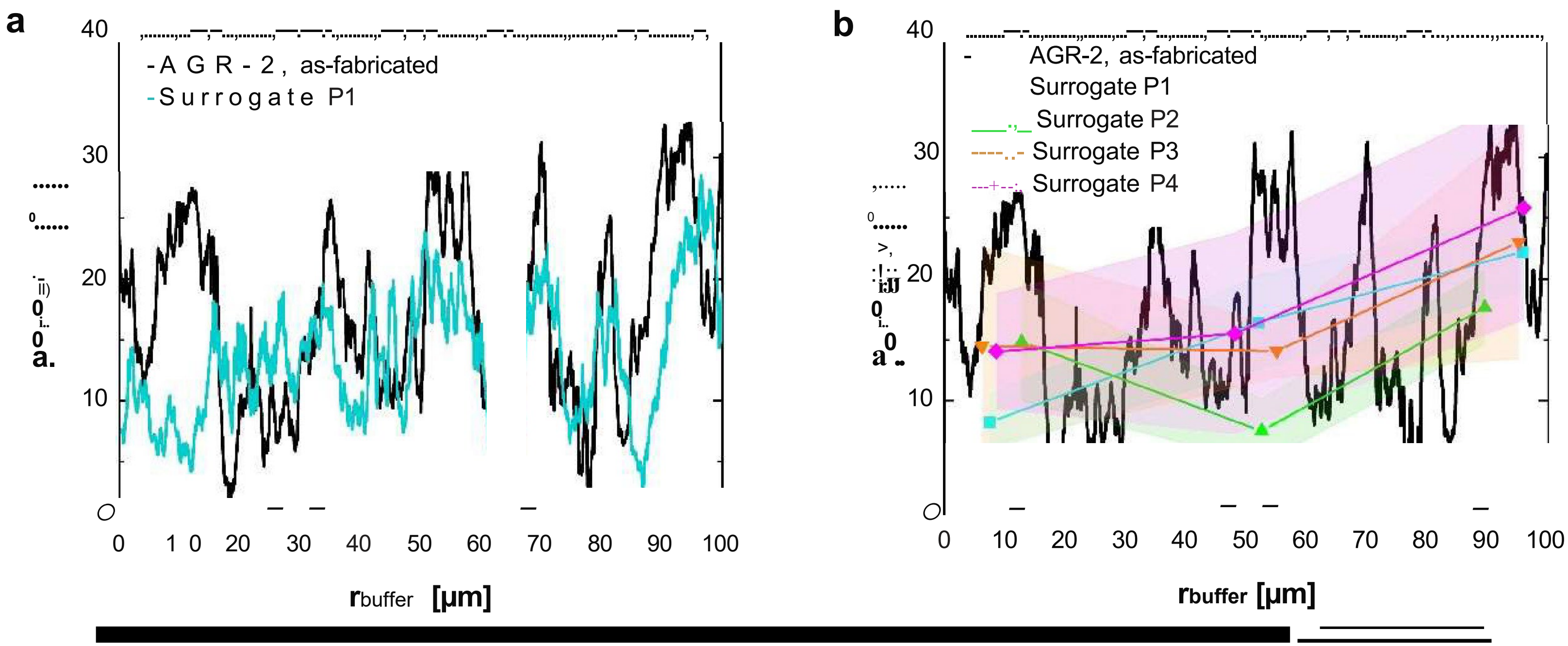

What buffer is

Isotropic pyrocarbon matrix
~60% density

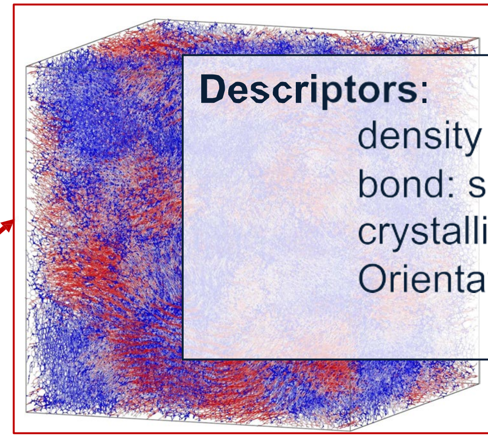

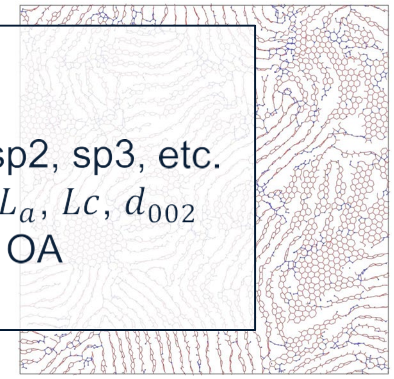

Descriptors:
- density
- bond: sp1, sp2, sp3, etc.
- crystallites: L_a, Lc, d_{002}
- Orientation: OA

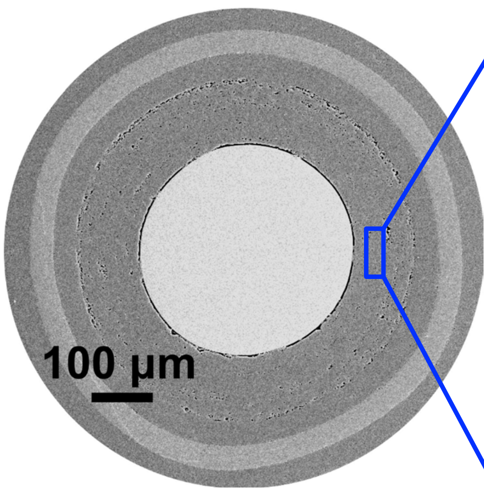

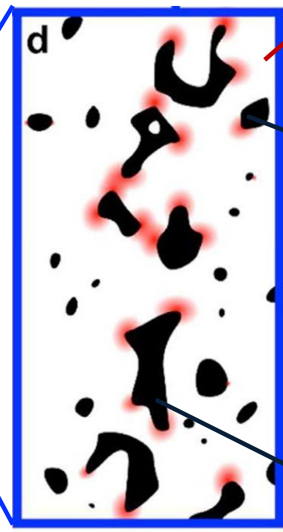

Small pores

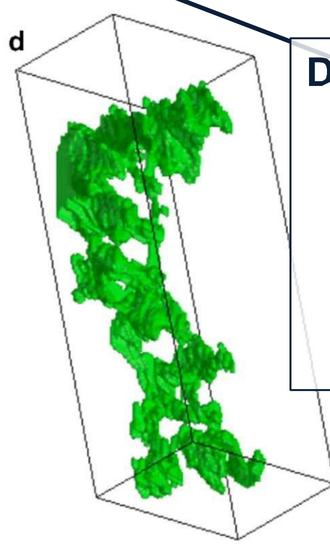

Descriptors:
- average porosity
- local fluctuation
- radial gradient
- *pore orientation?*
- *pore distribution?*

Large pores
Tangentially oriented

Microstructure descriptors of buffer

- Porosity parameters
  - average porosity
  - local fluctuation
  - radial gradient
  - *pore orientation?*
  - *pore distribution?*
- Matrix Parameters
  - density
  - bond: sp1, sp2, sp3, etc.
  - crystallites: L_a, L_c, d_{002}
  - Orientation: OA

Correlation analysis

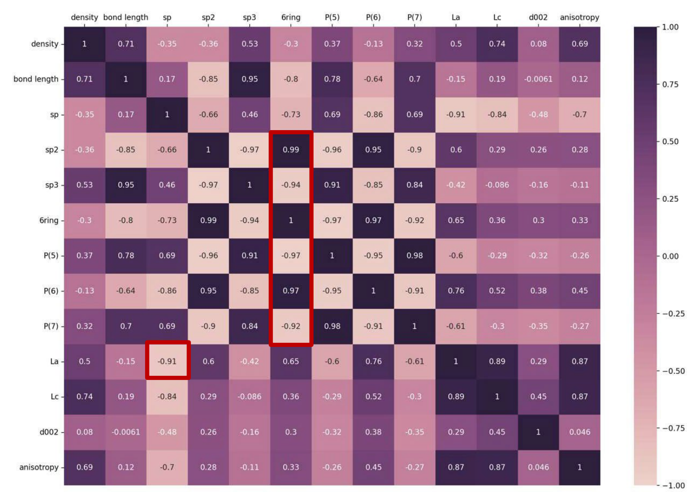

Microstructure-property

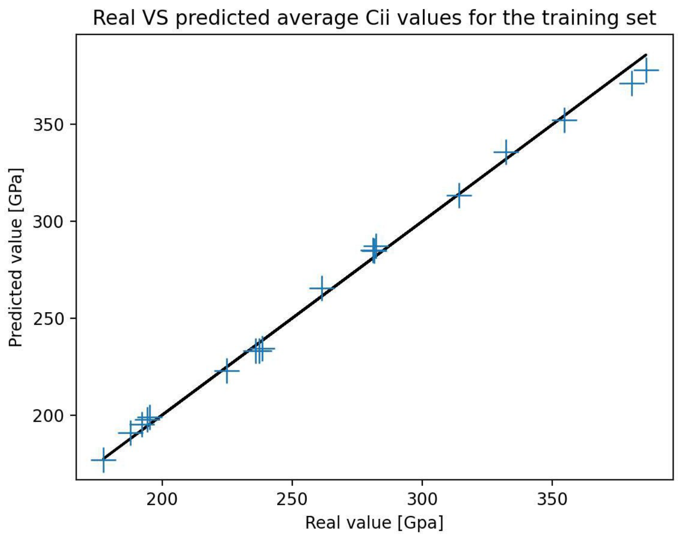

How does buffer porosity affect its fracture behavior?

- **Statistical BISON simulations of buffer fracture initiation and propagation**

  - *Masri et al. The role of heterogeneous porosity distribution on buffer fracture behavior in TRISO fuel particles (in preparation)*

Representation of buffer porosity in BISON

- Buffer porosity is randomly sampled with three parameters: **average porosity (A), radial gradient (B),** and **local fluctuation (Cξ)**, by fitting the experimental results using the below equation.
- The function is selected based on the assumption of constant mass deposition rate per unit radial length.
- Both elastic moduli and fracture stress are made dependent on porosity.

$$\eta(r) = A\left(1 - B\frac{r_0^2}{r^2}\right)(1 + C\xi)$$

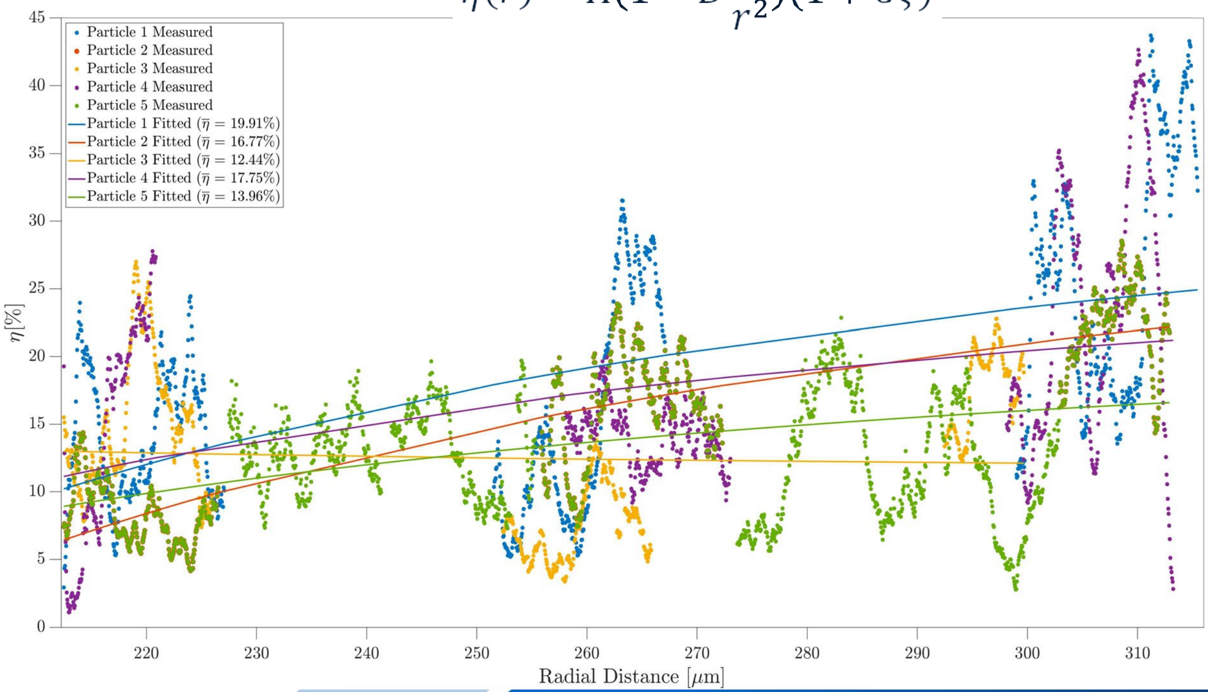

BISON: Williamson, R. L. et al., *J. Nucl. Mater.* 2012, *423* (1–3), 149–163.

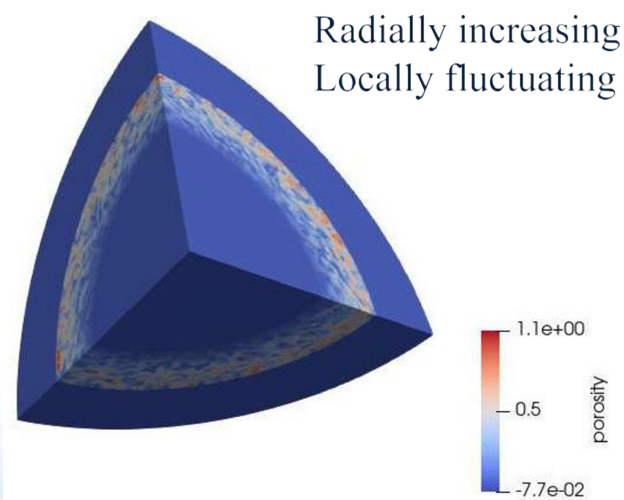

BISON simulations of buffer fraction: uniform porosity

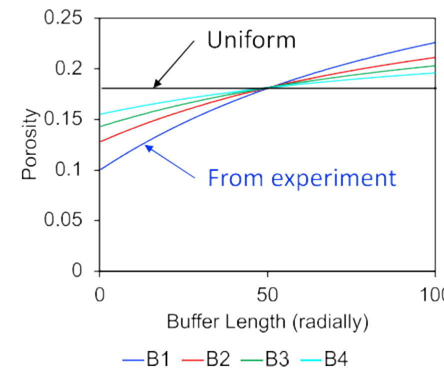

- Both elastic moduli and fracture stress are uniform
- Fracture is caused by **tangential stress**, not radial stress
- Fracture initiates from **kernel/buffer** interface
- Fracture propagates **radially**

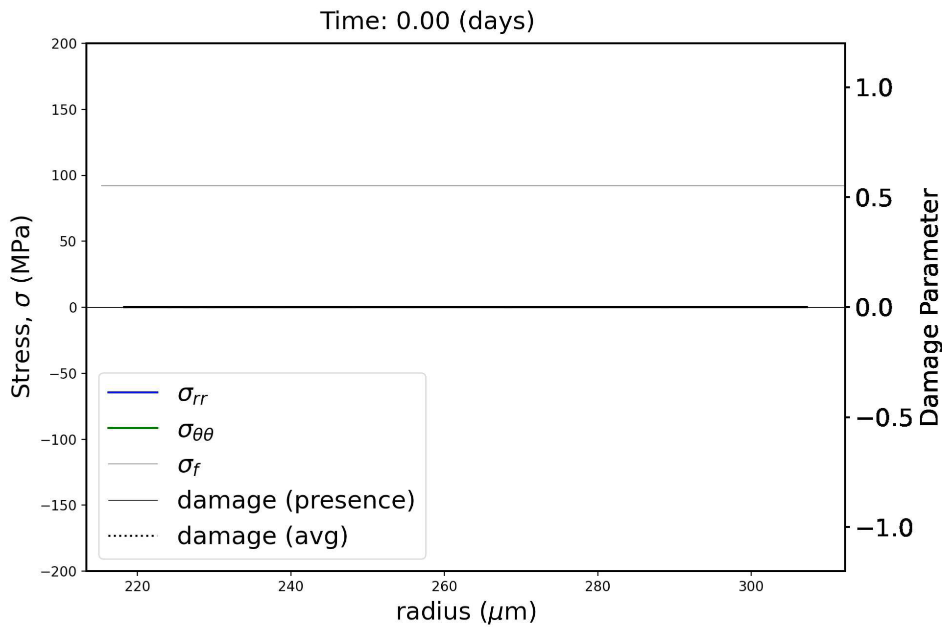

Color: stress
Black: crack

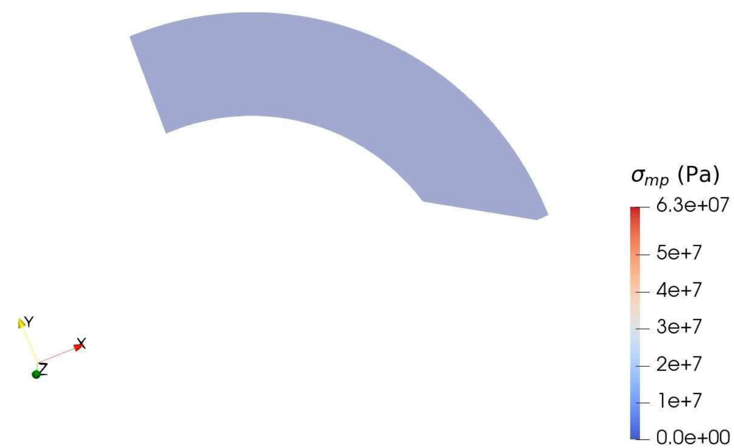

ADVANCED REACTOR TECHNOLOGIES PROGRAM

BISON simulations of buffer fraction: radially increasing porosity

- Both elastic moduli and fracture stress decrease radially
- Fracture is caused by **tangential stress**, not radial stress
- Fracture initiates from **buffer/IPyC interface**
- Radial crack connects with each other along tangential direction (**tearing**), instead of propagating radially

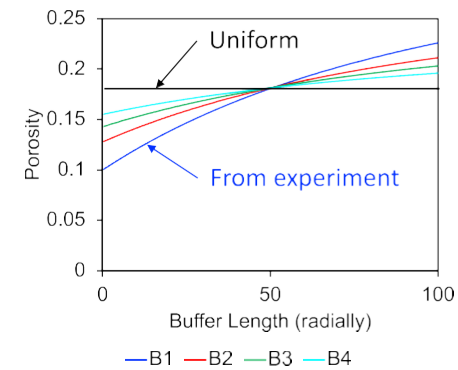

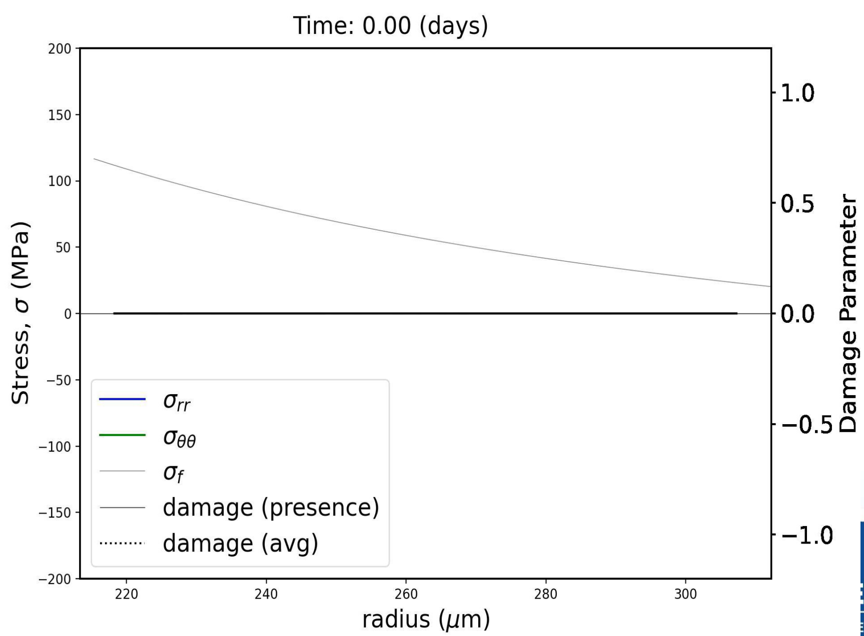

Color: stress
Black: crack

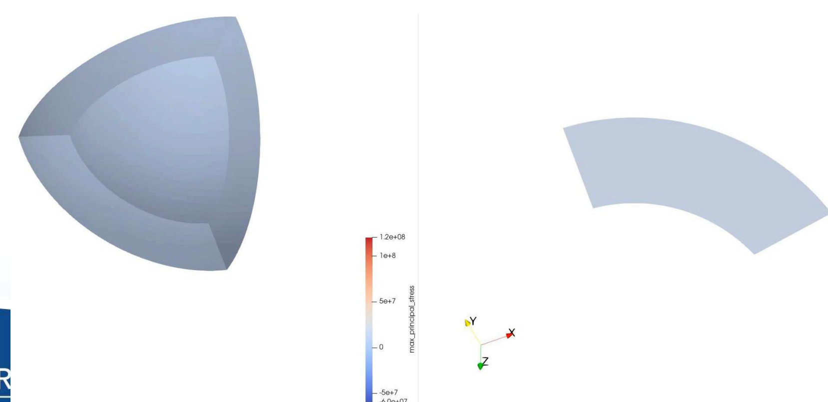

BISON simulations of buffer fracture: fracture initiation

- The fracture initiation point increases radially with the parameter B, which describes the rate of radial porosity increasement, implying the possibility of tailoring fracture by controlling porosity distribution.
- Local fluctuation in porosity induces some fluctuation in fracture initiation point.

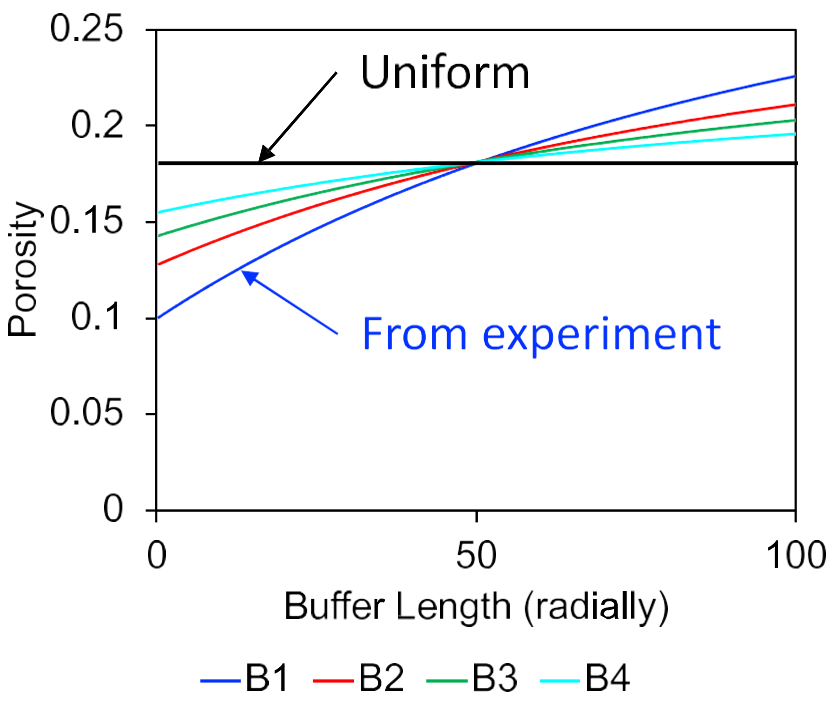

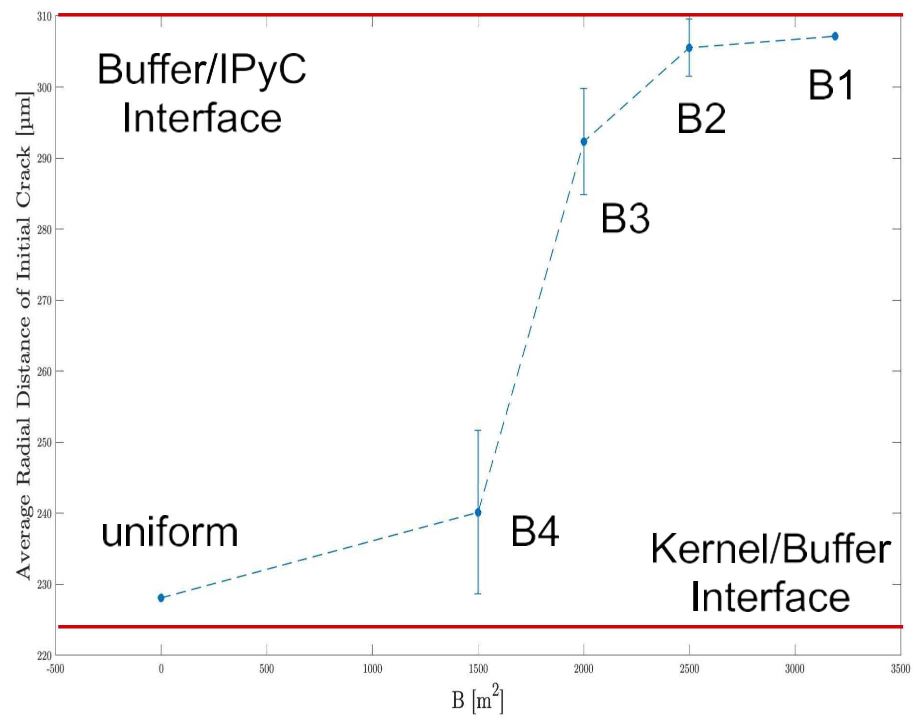

Irradiation induced changed in porosity and matrix microstructure

FIB-SEM, Raman, and TEM characterization

- C. *Griesbach, T. Gerczak,* C. *McKinney, Y. Zhang, R. Thevamaran, Irradiation-condition dependent mechanisms controlling buffer densification and fracture in TR/SO nuclear fuel particles, JNM, under review.*

Samples and irradiation condition

- Various irradiation conditions consider in terms of temperature and neutron fluence.
- **Porosity, solid fission products, densification,** and **fracture** are characterized.

5 – 4 – 2

compact

AGR-2 Irradiation Conditions

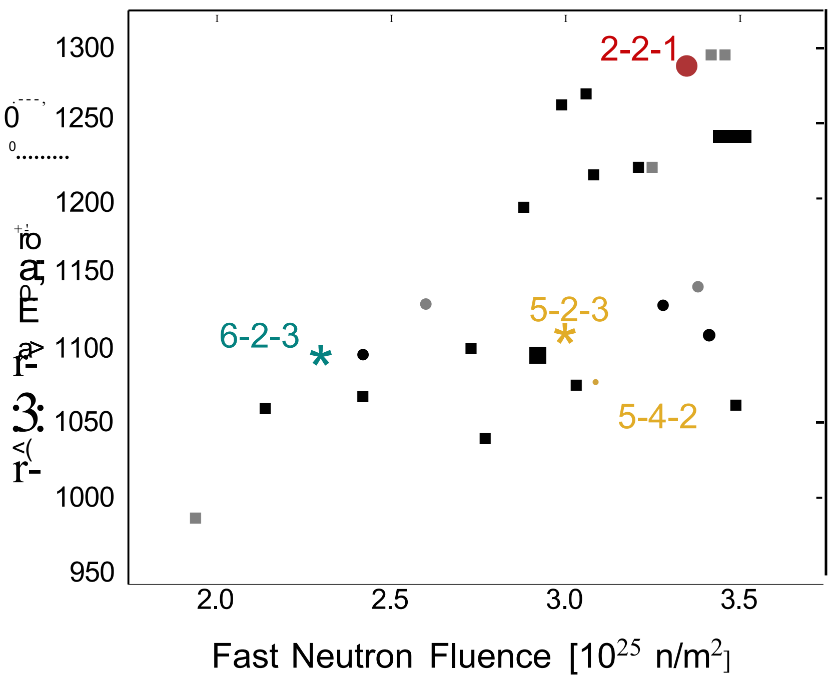

Compact	Mount	Particle	Ag (M_part/M_avg)	Temperature [OC]	Fluence [102s n/m2]	#full buffer scans	Raman	TEM
221	MM-D67	RS43	1.12	1287	3.35	2	X	X
221	MM-D67	RS46	1.8	1287	3.35	2		X
221	MM-D68	RS39	0.83	1287	3.35	1		
523	MM-D12	RS11	0.48	1108	3.00	1		X
523	MM-D12	RS28	0.43	1108	3.00	1		
542	MM-D55	RS25	1.59	1071	3.14	2	X	
623	MM-D69	RS18	1.87	1095	2.30	2		X
623	MM-D69	RS07	1.72	1095	2.30	1		X
623	MM-D70	RS35	0.81	1095	2.30	1	X	X
As fabricated AGR-2			*NIA*			1	X	X

Example: Capsule 2, high temperature and high fluence

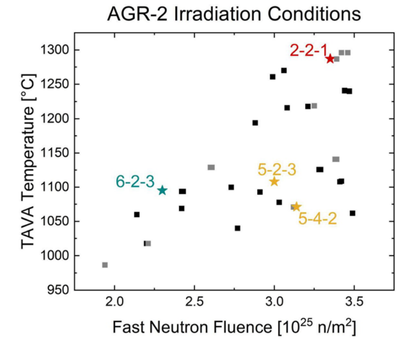

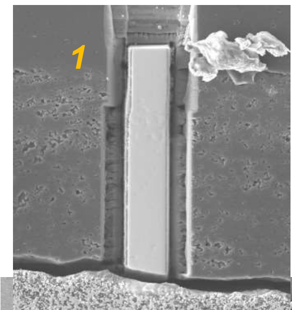

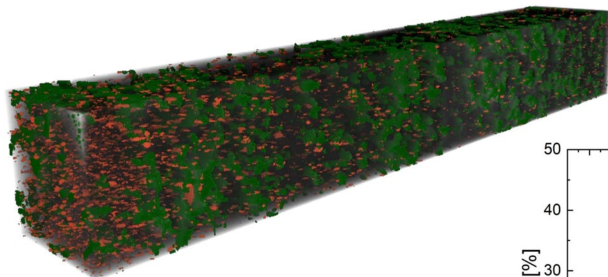

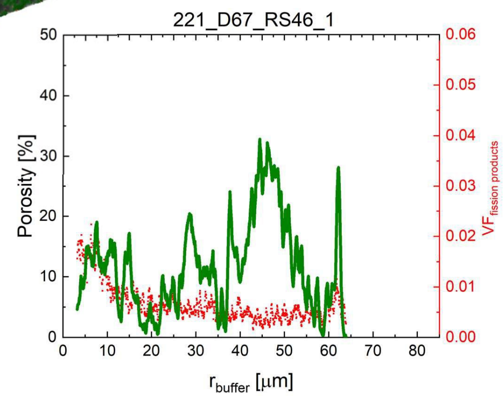

D67-RS46

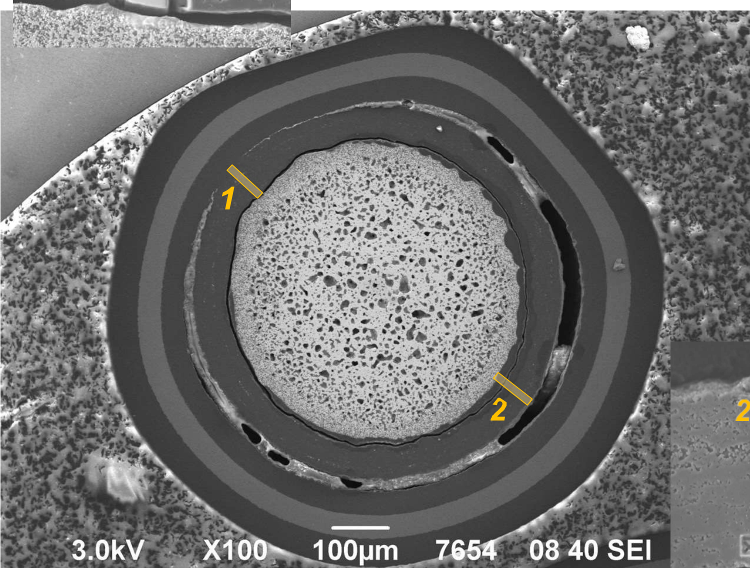

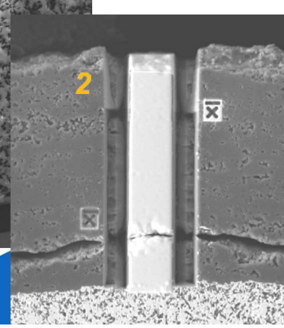

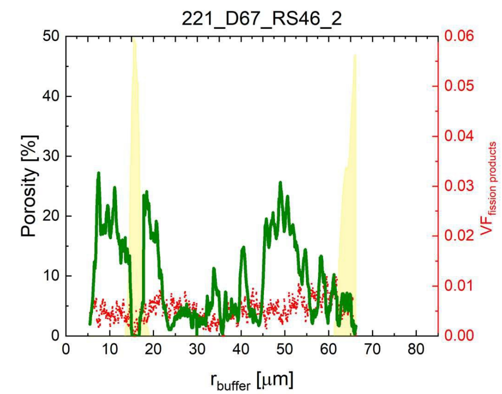

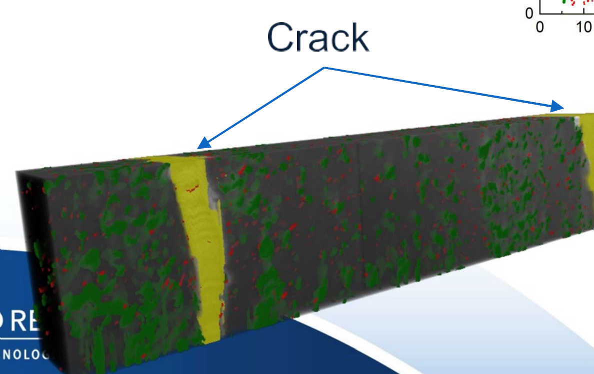

Change in porosity

- Irradiation reduces the average porosity and and changes the radial distribution due to concurrent pore closure induced by compressive stress and pore expansion due to fission gas.
- The change in radial gradient depends on temperature.

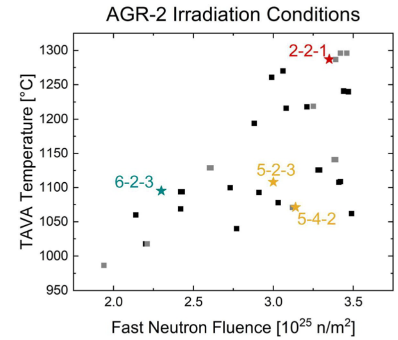

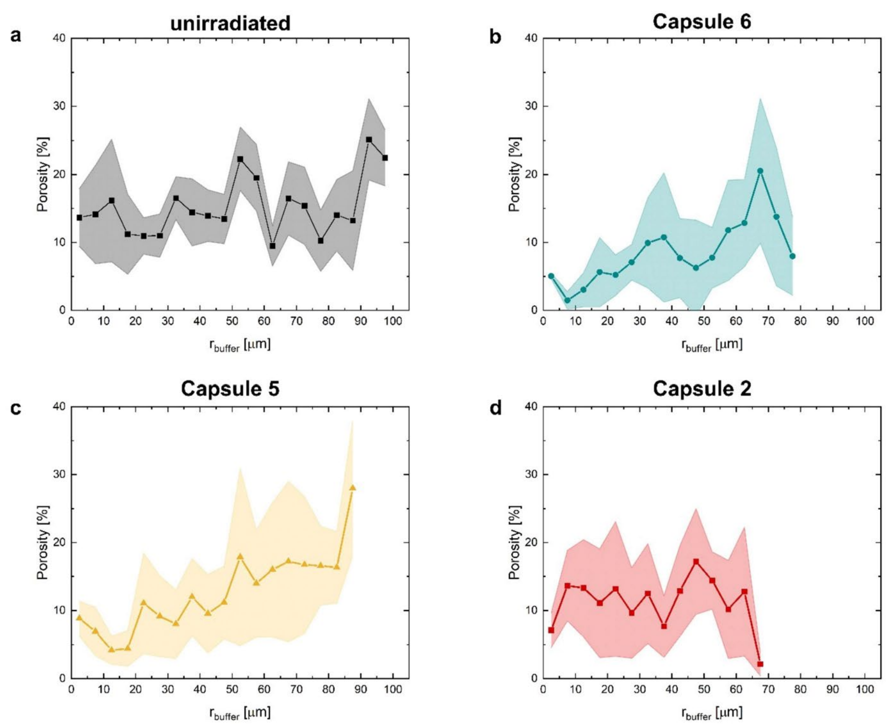

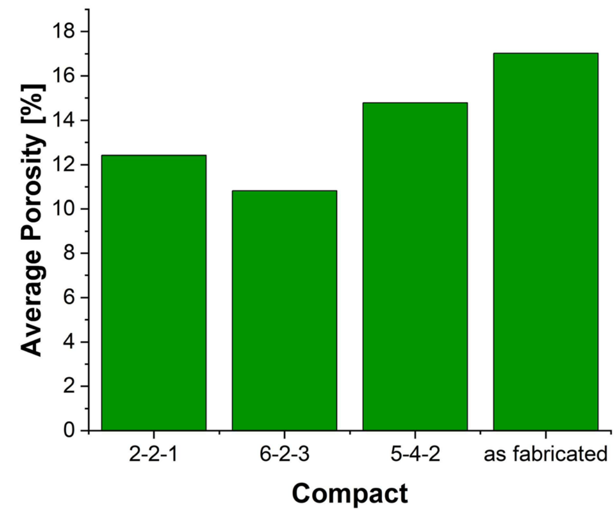

Change in matrix microstructure

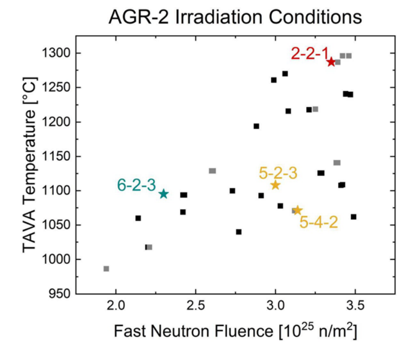

- Substantial densification that correlate positively with fluence and temperature has been observed.
- The matrix has experienced substantial graphitization as suggested by XRD and Raman analyses.
- Densification is dominated by change in matrix microstructure.

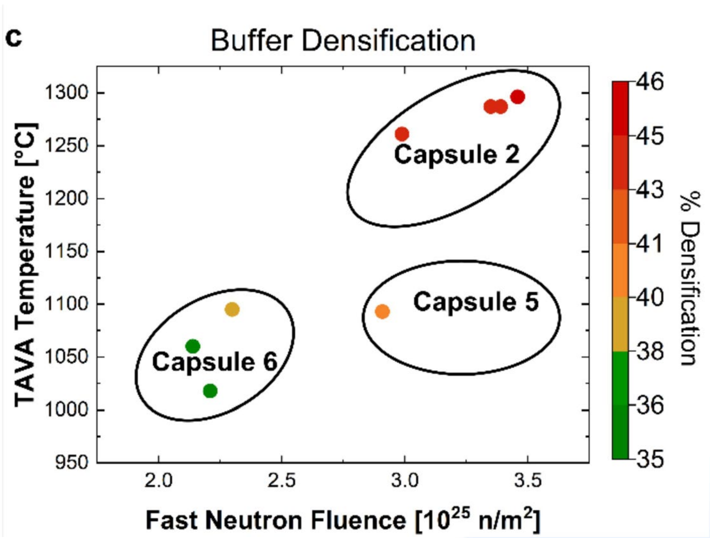

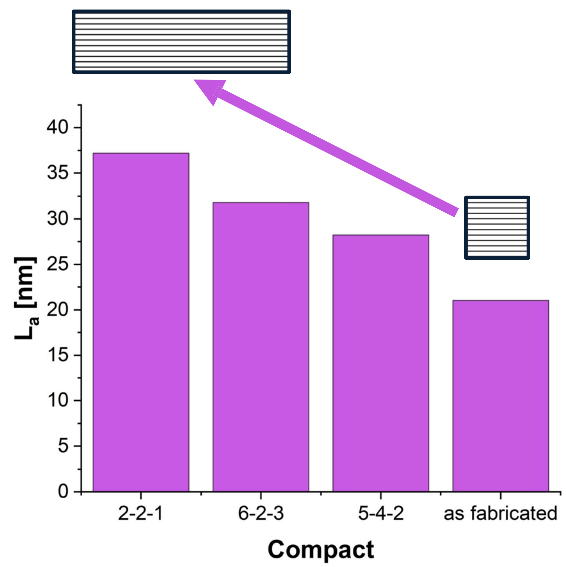

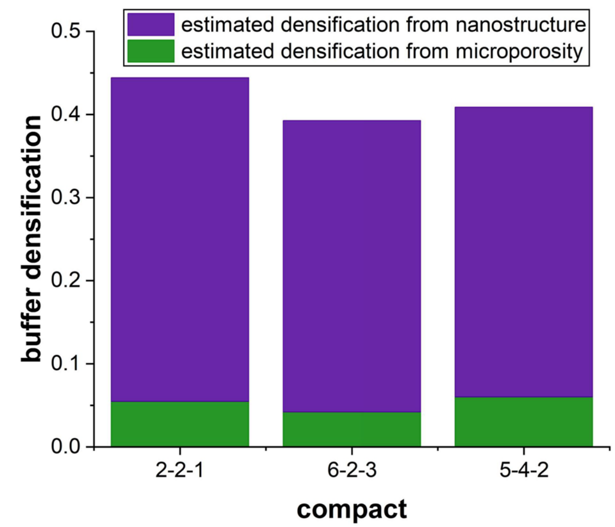

Fission products and radial fracture

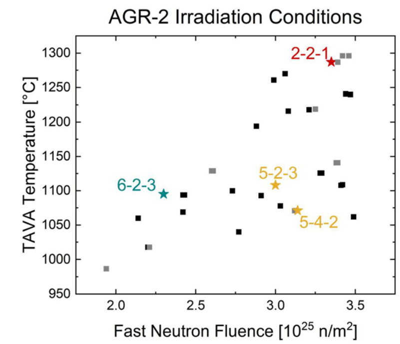

- High concentrations of solid fission products are recorded near the kernel in all particles.
- Both circumferential and radial fracture are identified in all three capsules, while the fraction of radial fracture increases with increasing fluence and decreases with increasing temperature.

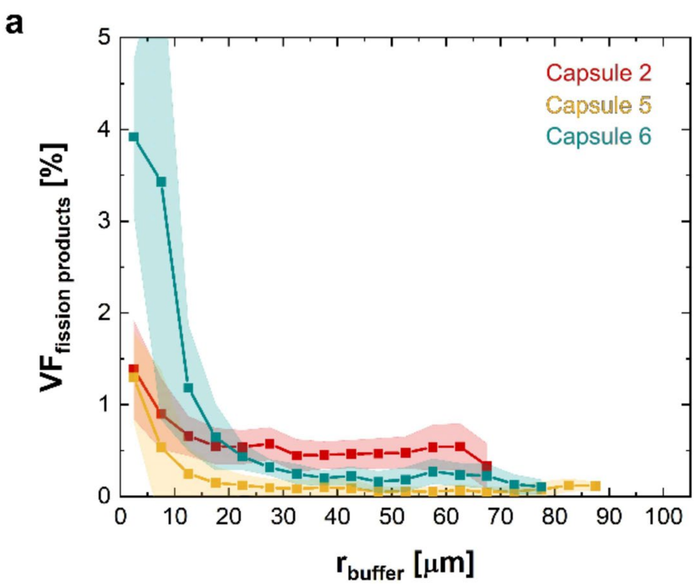

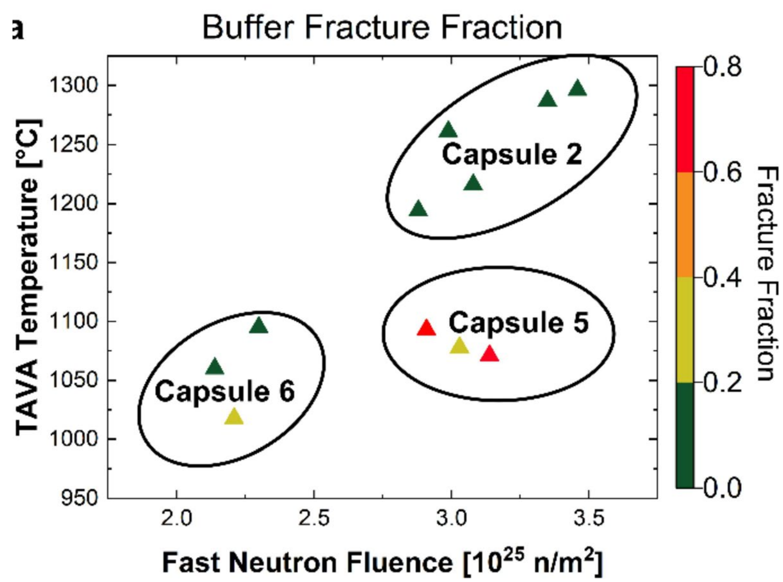

Unique mechanic properties of unirradiated buffer pyrocarbon

Nanoindentation and micro-compression

- C. *Griesbach, T. Gerczak, Y. Zhang, R. Thevamaran, Super elasticity and anisotropic mechanical response in porous pyrocarbon (in preparation)*

Super-elasticity revealed by nanoindentation and nano-pillar compression

- No failure or plasticity observed during in-situ nanoindentation.
- Brittle failure observed until 30% strain under micro-compression
- Radially compressed micro-pillar show lower yield strength than tangentially compressed.

(a) force-displacement curves from in situ SEM nanoindentation experiments with SEM images at select points during deformation in (a-1)- (a-3), (b) stress strain curves from in situ SEM micro compression experiments on the same sample compressed to ~10% strain without yielding (blue curve) and to ~30% strain exhibiting brittle failure; SEM images at select points during deformation in (b-1)- (b-3).

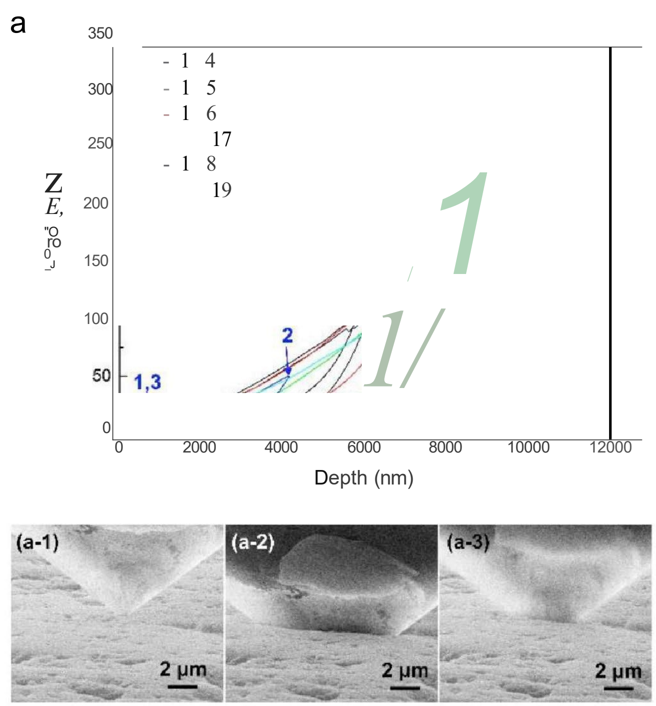

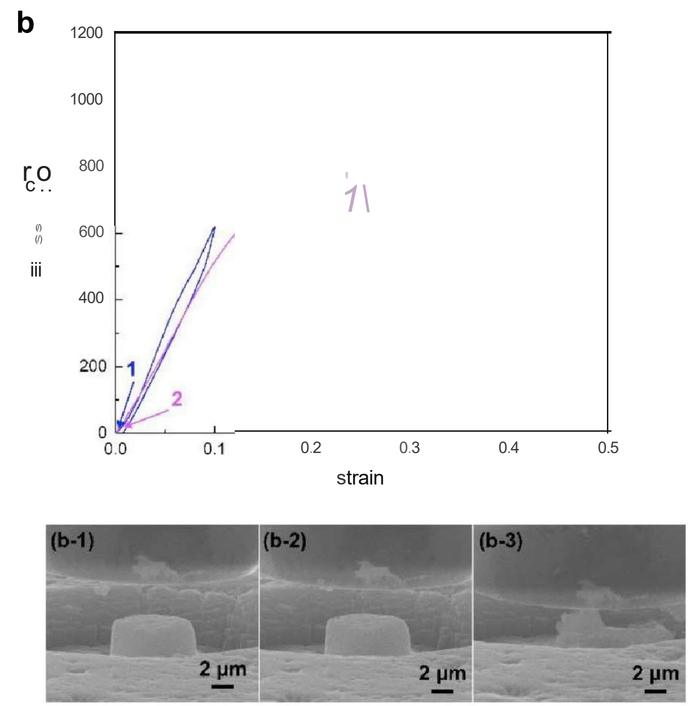

Unique deformation mechanisms

- Non-textured pyrocarbon can sustain large tensile and compressive strain.
- The elastic strain is accommodated by current curving of graphite planes normal to the loading direction and unfolding of graphite planes along the loading directions.
- Growth and coalescence of pre-existing nanoscale pores are responsible for eventual fracture.

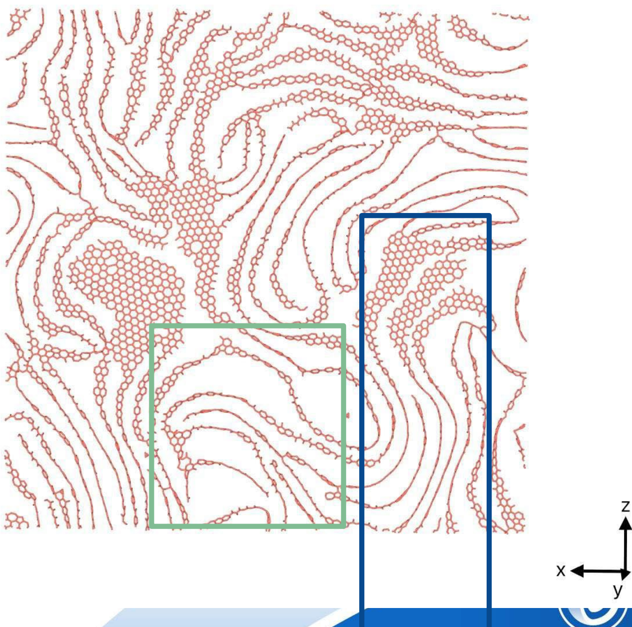

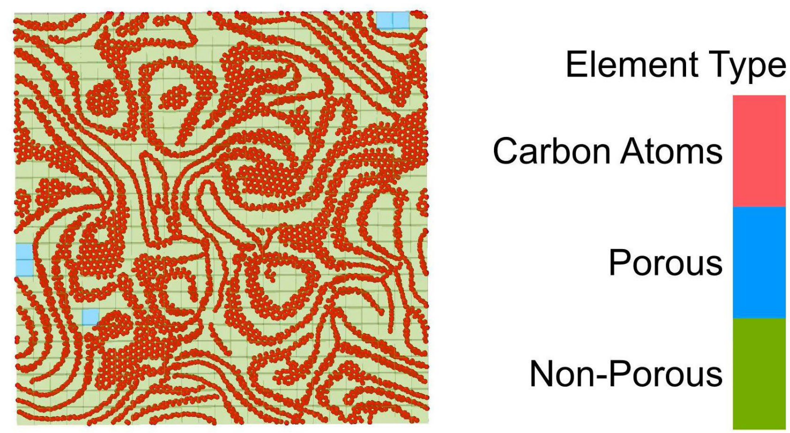

Summary

- Buffer consists of a low density pyrocarbon matrix (~58% theoretical density) and randomly distributed pores with a total volume of about 14%. The porosity increase radially and fluctuate locally.
- The radial porosity distribution strongly affects the fracture behavior of buffer.
- Irradiation causes significant densification and changes the total porosity, the porosity distribution, and the matrix microstructure. The densification is dominated by the graphitization of the pyrocarbon matrix.
- The unirradiated buffer pyrocarbon exhibits super-elasticity under compression owing to the unique deformation mechanisms.
- <u>The findings suggest that the fracture behavior of buffer depends critically on its microstructure (matrix + pore) that evolves with irradiation.</u>

Outlook

- Can we optimize the fracture behavior by controlling the initial buffer microstructure and porosity distribution?
  - ➢ Anisotropic pore distribution and mechanical properties
  - ➢ Atomic-scale mechanisms responsible for irradiation induced change in matrix microstructure and porosity distribution, which determine the transient mechanical properties
  - ➢ Progression of buffer fracture into SiC layer

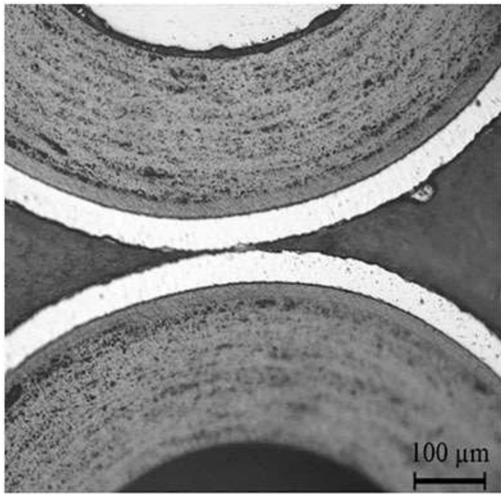

- Phase-II continuation awarded: PIIC-24-31266, Correlating buffer microstructure with failure progression into the SiC layer in TRISO (PI: Yongfeng Zhang; co-PIs: Ramathasan Thevamaran, Tyler Gerczak, Wen Jiang (NCSU))
- In general, accurately quantifying changes in microstructure and mechanical properties of pyrocarbon is needed for improving the irradiation performance of TRISO particles.

Thank you!

GAS-COOLED REACTOR

ADVANCED REACTOR TECHNOLOGIES PROGRAM

U.S. DEPARTMENT OF ENERGY